Laboratory Investigation (2005) 85, 512–521

www.laboratoryinvestigation.org

Inhibition of TGF-β modulates macrophages and vessel maturation in parallel to a lowering of interstitial fluid pressure in experimental carcinoma

Alexei V Salnikov[1], Pernilla Roswall[2], Christian Sundberg[1], Humphrey Gardner[3], Nils-Erik Heldin[2] and Kristofer Rubin[1]

[1]*Department of Medical Biochemistry and Microbiology, Uppsala University, Uppsala, Sweden;* [2]*Department of Genetics and Pathology, Rudbeck Laboratory, Uppsala, Sweden and* [3]*Department of Research Pathology, Biogen Idec Inc., Cambridge, MA, USA*

A pathologically elevated interstitial fluid pressure (IFP) is a characteristic of both clinical and experimental carcinoma. The soluble TGF-β receptor type II-murine Fc:IgG_{2A} chimeric protein (Fc:TβRII) lowers IFP in the KAT-4 experimental model for anaplastic thyroid carcinoma. Analyses of messenger RNA (mRNA) expressions by Affymetrix microarrays and RNase protection assays, as well as of protein expressions identified tumor macrophages as targets for Fc:TβRII. Treatment with Fc:TβRII reduced albumin extravasation, increased coverage of α-smooth muscle actin-positive cells and reduced expression of NG2, a marker of activated pericytes, in KAT-4 carcinoma blood vessels. Specific inhibition of interleukin-1 (IL-1), a major cytokine produced by activated macrophages, lowered carcinoma IFP to a similar degree as Fc:TβRII but had no significant effect on the parameters of blood vessel maturation. Neither Fc:TβRII nor inhibition of IL-1 changed blood vessel density. Finally, pretreatment of KAT-4 carcinomas with Fc:TβRII increased the antitumor efficacy of doxorubicin. Our data emphasize a potential role of tumor macrophages in carcinoma physiology and identify these cells as potential stromal targets for treatment aimed to improve efficacy of chemotherapy.
Laboratory Investigation (2005) **85,** 512–521, advance online publication, 14 February 2005; doi:10.1038/labinvest.3700252

Keywords: anaplastic thyroid carcinoma; growth factors; interleukins; vasculature; xenograft tumors; soluble receptors

Resistance of tumors to chemotherapy can in part be explained by impaired delivery of chemotherapeutic agents into the tumor tissue.[1] The pathologically elevated interstitial fluid pressure (IFP), a characteristic of solid malignancies, reflects a barrier for drug transport into tumors.[2–7] An increased IFP reduces the transcapillary pressure gradient driving outward fluid flux over the capillary wall.[8]

Rapid and transient lowering of IFP in experimental carcinoma increases convective transport of low molecular mass compounds into the carcinoma tissue, as well as efficacy of chemotherapy during the time period of lowered tumor IFP.[5–7] Long-term treatment with inhibitors of the platelet-derived growth factor (PDGF),[9] vascular endothelial growth factor (VEGF)[10] systems or with dexamethasone[11] lowers tumor IFP in several experimental carcinoma models. Lowering of tumor IFP by inhibition of PDGF parallels an increased uptake of and sensitivity to cytostatic drugs.[12,13] Furthermore, lowering of tumor IFP by treatment with a specific inhibitor of VEGF paralleled the increased efficacy of conventional chemotherapy for human rectal carcinoma.[14] Thus, available data suggest that enhancement of drug delivery to solid malignancies by reduction of tumor IFP constitutes an attractive modality to augment efficacy of conventional chemotherapy. The pathogenic mechanisms involved in the generation of the high tumor IFP are not fully known although several mechanisms have been suggested (for a recent review, see Heldin *et al*[15]).

TGF-β is believed to play a dual role during the progression of carcinoma towards a malignant

Correspondence: Professor K Rubin, PhD, Department of Medical Biochemistry and Microbiology, Uppsala University, BMC, Box 582, SE-751 23 Uppsala, Sweden.
E-mail: Kristofer.Rubin@imbim.uu.se
Received 10 October 2004; revised 20 December 2004; accepted 21 December 2004; published online 14 February 2005

metastatic phenotype;[16] during early stages, negatively controlling carcinoma cell proliferation and at later stages promoting metastases. Long-term presence of Fc:TβRII suppresses metastasis formation in experimental tumor models.[17,18] Treatment of xenograft human KAT-4 anaplastic thyroid carcinoma in mice with a soluble TGF-β receptor type II-murine Fc:IgG_{2A} chimeric protein (Fc:TβRII) lowered tumor IFP in a dose- and time-dependent manner.[19] The present study was initiated to delineate potential mechanisms by which Fc:TβRII reduced KAT-4 carcinoma IFP. KAT-4 carcinomas were chosen since they are well characterized and cultured KAT-4 carcinoma cells are refractory to TGF-β.[19]

Materials and methods

Reagents

The TGF-β receptor type II-murine Fc:IgG_{2A} chimeric protein (Fc:TβRII) has been described previously.[20] Human interleukin-1 receptor antagonist (rh-IL-1 Ra; Kineret) was from Amgen (Louisville, KY, USA). Anti-mouse CD31/PECAM-1 monoclonal antibody (Mab), biotin anti-mouse panendothelial cell antigen Mab, anti-mouse Ly-6G and Ly-6C (Gr-1) (RB6-8C5) Mab and FITC-conjugated anti-mouse I-A/I-E (2G9) Mab were from BD PharMingen (San Diego, CA, USA). Rat anti-mouse F4/80 Mab was from Serotec (Oxford, UK). Goat anti-actin (I-19) IgG was from Santa Cruz Biotechnology (Santa Cruz, CA, USA). Rabbit polyclonal anti-laminin IgG and FITC-conjugated mouse anti-α smooth muscle actin (αSMA) Mab (clone 1A4) were from Sigma (St Louis, MO, USA), rabbit polyclonal anti-NG2 IgG was from Chemicon (Temecula, CA, USA), Alexa Flour 488 goat anti-rabbit IgG (H + L) and Alexa Fluor 594 goat anti-rat IgG (H + L) were from Molecular Probes (Eugene, OR, USA). Tumor cells were visualized with rabbit anti-TPA:B1 IgG (Sangtec Medical AB, Bromma, Sweden). Anti-mouse LYVE-1 IgG detecting lymphatic vessel endothelial HA-receptor-1 and anti-mouse VEGFR-3 (AFL-4) Mab were kindly supplied by Dr Kari Alitalo (University of Helsinki, Finland). Human and murine VEGF ELISA kits were from R&D Systems (Abingdon, Oxon, UK).

Tumors and Treatments

KAT-4 anaplastic thyroid carcinoma cells[21] were injected subcutaneously (s.c.) in the left flank of athymic C57 bl/6 mice as described.[19,22] After 6–10 weeks, mice with size-matched KAT-4 tumors (approximately 0.5–1 cm^3) received Fc:TβRII, IgG_{2A} or rh-IL-1 Ra. Fc:TβRII or IgG_{2A} was given as a single intravenous (i.v.) dose of 10 mg/kg. Tumors were excised and investigated after 10 days. rh-IL-1 Ra (7.5 mg/injection) was administered s.c. twice daily for 10 days.

Doxorubicin (Adriamycin, Pharmacia, Stockholm, Sweden) was given intraperitoneally (i.p.) at a dose of 3 mg/kg every second day during a 2-week period, starting 10 days after administration of a single dose of Fc:TβRII (1 mg/kg) or IgG_{2A} to KAT-4 carcinoma-bearing mice. Control animals received a single injection of Fc:TβRII at a dose of 1 mg/kg. The effect of treatment was assessed by evaluating the size of tumor viable tissue at the end point of the experiment. The relative size of tumor viable tissue was measured on representative tumor sections using the NIH Image 1.62 software. Evaluation of the relative size of viable tumor tissue gave more accurate data on antitumor effects of treatment than external size measurements due to morphology of KAT-4 tumors.

Tumor IFP was measured by the 'wick-in-the needle' technique as described.[5] All animal experiments were approved by the Ethical Committee for Animal Experiments in Uppsala (Sweden). The number of animals was minimized to comply with guidelines from the Ethical Committee.

Affymetrix Microarrays

Total RNA was extracted from KAT-4 carcinomas using a LiCl/Urea-method.[23] Preparation of labeled cRNA probe was performed according to recommendations from Affymetrix Inc. Poly(A) messenger RNA (mRNA) was isolated and used as template for double-stranded cDNA synthesis with an oligo(dT)24 primer containing a T7 RNA polymerase promoter site added to the 3′ end. The cDNA was extracted with phenol–chloroform, ethanol-precipitated, and used as a template for *in vitro* transcription with biotin-labeled nucleotides. Labeled cRNA was fragmented and a hybridization mix was generated. Aliquots of each sample (10 μg cRNA in 200 μl hybridization mix) were hybridized to a Gene-chip Mu74Av2 array. Scanned files in the 'Cel' format from arrays lacking significant artifacts were exported to the Rosetta Resolver software suite. Intensity ANOVA analysis was performed to reveal transcripts with differences in expression between treated with Fc:TβRII or IgG_{2A} groups with $P \leq 0.05$.

Morphological Analyses

Immunohistochemistry and double immunofluorescence stainings of cryosections were performed as previously described.[24,25] The density of macrophages and granulocytes was determined using a counting grid (15–34 vision fields, $\times 500$). Results are expressed as cell density per mm^2 of the tumor viable zone and as a percent of total cellular density. Analyses by confocal microscopy were made with a Leica TCS SP spectral confocal microscope (Leica Microsystems Heidelberg GmbH).

In Vivo Perfusion and Permeability Assay

After treatment with Fc:TβRII, IgG_{2A} or rh-IL-1 Ra perfused tumor vessels were visualized using FITC-Dextran (mean molecular mass 2000 kDa; Sigma). Vascular permeability was assessed by determining Evans blue dye (EBD) leakage into the tumor interstitium. EBD (Sigma, 30 mg/kg) was administered i.v. 30 min and FITC-Dextran (100 mg/kg) 2 min before killing an animal. To evaluate perfused area of tumor vasculature and leakage of EBD, either 50 μm formalin-fixed tissue sections were analyzed by confocal microscopy or 20 μm frozen sections by fluorescent microscopy. Vascular leakage was quantified based on the amount and distribution of extravasated EBD and was graded from 0 to $+++$. Data were dichotomized into two groups: one low leakage group (0 and $+$) and one high leakage ($++$ and $+++$). Data are presented as percentage of vessels with high leakage for EBD in 12 fields of vision from six sections per tumor taken 100 μm apart and assessed under low magnification. The extent of EBD leakage was analyzed by densitometry using the NIH Image 1.62 software. Digital images were analyzed in a gray-scale mode and dye density in tumor sections presented as number of pixels per area of tumor tissue.

Immunoblot Analysis

Viable parts of KAT-4 tumors were dissected out and lysed as previously described.[19] The pellet (25 000 *g*) of insoluble cellular components from the lysis was subjected to sonication in 50 mM Tris HCl pH 7.4, 5 mM EDTA and 1% sodium dodecylsulfate. Immunoblot analyses were performed as previously described,[19] on both cell fractions using the anti-NG2 or anti-αSMA antibodies. The second solubilization appeared to contain approximately 70–80% of the specific signal in the NG2 immunoblots.

RNase Protection Assay

Total RNA was extracted from tumor tissues as described above. RNase protection assay (RPA) was performed using BD RiboQuant Multi-Probe RPA System kits (mCK-2b, mAngio-1 and hAngio-1) (BD Biosciences). The mRNA expression levels were measured using a Phosphor Imager (Fuji 2000, Fuji, Tokyo, Japan). The levels were normalized to L32 (mouse) or GAPDH (human) housekeeping genes and presented as relative mRNA expression.

Determination of VEGF Protein Level in KAT-4 Tumors

Specimens from the viable zone of KAT-4 tumors were extracted (1:10 w/v) in 50 mM Tris-HCl pH 7.5, 5 mM EDTA, 1 M NaCl, 1% NP-40, 0.26% Na-deoxycholate, 50 mM NaF, 50 mM β-glycerophosphate and protease inhibitors, homogenized by freeze-thawing and cleared by centrifugation at 17 000 *g* for 20 min. A volume of 1 M NaCl was used to extract VEGF bound to heparan sulfate proteoglycans in the extracellular matrix (ECM) or cell surfaces. Supernatants were diluted five times with 10 mM Tris-HCl prior to measurements. Total protein concentration in the specimens was determined using the bicinchoninic acid protein assay (BCA, Pierce, Rockford, IL, USA) and VEGF determined using a commercial ELISA kit (R&D Systems).

Statistical Methods

The unpaired, two-tailed Student's *t*-test and the Mann–Whitney *U*-test were used. $P<0.05$ was considered statistically significant. Standard deviations of data points are indicated in the figures.

Results

Fc:TβRII Downregulates Genes Expressed by Macrophages

Available data suggest that treatment with Fc:TβRII modifies host rather than carcinoma cell activity in KAT-4 tumors.[19] Expression of mouse (host) genes was investigated by mouse Affymetrix microarray analyses. Differences in gene expressions in carcinomas from animals treated with Fc:TβRII ($n=3$) or IgG_{2A} ($n=3$) were compared. A set of 281 genes out of the totally $\sim 1.25 \times 10^4$ genes presented on the chips were significantly changed ($P<0.05$; ANOVA). Of these genes, 41 were either upregulated by $\geq 100\%$ or downregulated by $\geq 50\%$ (Table 1).

Several genes known to be expressed by macrophages were significantly downregulated after treatment with Fc:TβRII (Table 1). These genes included S100 calcium-binding protein A9, major histocompatibility complex (MHC) class II antigens, mannose receptors, IL-1β and monocyte chemotactic protein-2 (MCP-2). Most of the highly expressed genes encoding ECM proteins were not regulated in KAT-4 carcinomas subjected to TGF-β1 and -β3 inhibition, for example, genes encoding interstitial collagens (data not shown). The only ECM protein that was significantly downregulated was the small leucine-rich repeat proteoglycan, fibromodulin. Genes encoding the hemoglobin A- and B-chains were most markedly upregulated. The significance of the latter finding is unclear.

RPA and immunofluorescence stainings were performed to validate the microarray results. RPA of several mouse cytokine genes revealed a specific downregulation of IL-1β and IL-1Ra (Figure 1a). The IL-1Ra gene was not included in the microarrays. In agreement with the microarray data, quantitative morphological analyses showed that the number of macrophages was reduced by around 30% in tumors treated with Fc:TβRII ($n=5$) compared to control

Table 1 Changes in gene expression in xenografted human anaplastic thyroid carcinoma after inhibition of TGF-β1 and -β3

Accession no.	*Description*	*Fold change*	*Intensity*	
			1	*2*
Immune system associated genes				
M83219	S100 calcium-binding protein A9	−4.16	0.61	0.15
U35330	Histocompatibility 2, class II, locus Mb1	−3.73	0.47	0.13
M21932	Histocompatibility 2, class II antigen A, beta 1	−3.62	5.49	1.54
AB023418	MCP-2/CCL8	−3.09	9.15	3
L43371	Hydrogen peroxide inducible protein 53	−2.7	0.33	0.12
M15131	Interleukin 1 beta	−2.68	0.33	0.13
U35330	Histocompatibility 2, class II, locus Mb1	−2.63	1.17	0.45
X12905	Properdin factor, complement	−2.46	1.17	0.48
M23158	Leukocyte common antigen, exon 33	−2.18	0.27	0.12
Z11974	Mannose receptor, C type 1	−2.11	1.42	0.68
Vasculature associated genes				
X59556	Endothelin 2	2.34	0.12	0.29
Growth factors				
AJ009862	Transforming growth factor, beta 1	−2.2	0.81	0.38
AF100906	Bone morphogenetic factor 11 (Bmp11)	2.26	0.13	0.29
Enzymes and metabolism				
AI181346	Carboxylesterase 3	2.21	0.13	0.28
AV086797	Creatine kinase, muscle	2.27	0.29	0.68
AF029843	Phosphoglycerate mutase 2	2.37	0.13	0.3
Receptors				
M34476	Retinoic acid receptor, gamma	−2.41	0.3	0.13
AF016271	Cadherin 16	2.03	0.12	0.25
D13517	Asialoglycoprotein receptor 1	2.37	0.13	0.3
Others				
M13805	Mouse type I epidermal keratin mRNA, clone pkSCC-50, 3′ end	−5.27	0.65	0.13
U51112	Solute carrier family 9 (sodium/hydrogen exchanger), member 1	−4.52	0.55	0.12
U15784	Src homology 2 domain-containing transforming protein C1	−2.82	0.34	0.12
U68058	Frizzled-related protein	−2.3	0.29	0.13
M13805	Mouse type I epidermal keratin mRNA, clone pkSCC-50, 3′ end	−2.19	2.31	1.07
AW050325	Crystallin, lambda 1	−2.11	0.99	0.48
U70132	Paired-like homeodomain transcription factor 2	−2.06	0.25	0.12
AF002283	Actinin alpha 2 associated LIM protein	2.01	0.12	0.25
AB013345	Potassium channel, subfamily K, mem. 3	2.04	0.13	0.27
M30774	Thymidylate synthase pseudogene	2.08	0.21	0.45
C76643	DNA segment, Chr 15, ERATO Doi 30	2.12	0.14	0.31
AV229143	Interferon activated gene 202A	2.13	0.21	0.45
U10341	A kinase (PRKA) anchor protein 4	2.16	0.12	0.26
V00714	Hemoglobin alpha, adult chain 1	2.2	6.59	14.71
AB019558	Parkin	2.21	0.18	0.41
AV330895	Ubiquintin c-terminal hydrolase related polypeptide	3.2	0.12	0.4
J00413	Hemoglobin, beta adult major chain	3.38	7.51	25.72
AJ002522	Myosin, heavy polypeptide 1, skeletal muscle, adult	4.44	0.29	1.3
ESTs				
AW125849	ESTs	−2.37	0.42	0.18
AI196645	ESTs	−2.15	1.46	0.69
AW125480	ESTs	2.02	0.83	1.7
AW120925	ESTs	2.18	0.16	0.35

Affymetrix microarrays encompassing $\sim 1.25 \times 10^4$ mouse genes were hybridized with mRNA from KAT-4 carcinomas treated with Fc:TβRII ($n=3$) or with IgG_{2A} ($n=3$). A set of 41 genes that fulfilled the following two criteria are listed: significant up- or downregulation between the two groups ($P<0.05$; ANOVA); and upregulation by $\geq 100\%$ or downregulation by $\geq 50\%$.

tumors treated with IgG_{2A} ($n=5$; $P<0.0026$) (Figure 1b). The microarray analyses showed a particularly strong downregulation of mRNAs encoding MHC class II antigens (Table 1). Expression of MHC class II antigens in KAT-4 carcinoma was largely restricted to a subset of F4/80-positive macrophages (Figure 1d). CD31-positive vessels expressing MHC class II antigens could not be positively identified. Double immunofluorescence and confocal analyses revealed that $54 \pm 15\%$ of F4/80-positive macrophages were also positive for MHC class II antigens in control tumors (Figure 1c) but only $16 \pm 3\%$ in

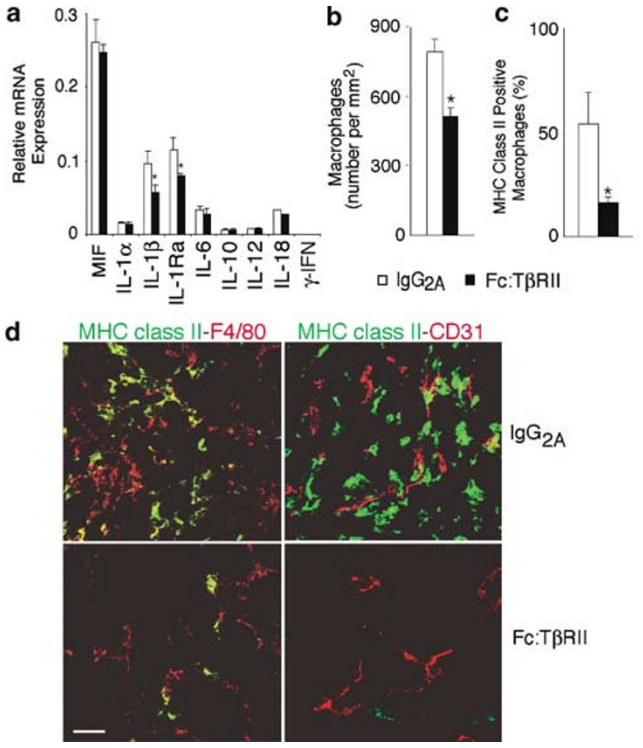

Figure 1 Fc:TβRII modulated macrophages in KAT-4 carcinomas. Expression of a set of cytokine mRNAs in KAT-4 carcinomas treated with Fc:TβRII ($n=3$) or IgG_{2A} ($n=3$). (**a**) Carcinoma RNA was extracted 10 days after a single injection of Fc:TβRII (10 mg/kg) or IgG_{2A} (10 mg/kg) and samples were subjected to RPA. (**b**) Density of F4/80-positive tumor macrophages in KAT-4 carcinomas treated with Fc:TβRII (filled bars, $n=5$) or IgG_{2A} (open bars, $n=5$). In (**c**) and (**d**), double immunofluorescence stainings and confocal analyses were used to evaluate and quantify the expression of MHC class II antigens (green) by F4/80-positive intratumoral macrophages or CD31-positive endothelial cells (red). In (d) yellow color identifies a subset of F4/80-positive macrophages expressing MHC class II antigens (left panel) or expression of MHC class II antigens by CD31-positive endothelial cells (right panel). Representative pictures from four to five tumors per experimental group are shown. Bar, 40 μm. * indicates $P<0.05$ from IgG_{2A} controls.

tumors treated with Fc:TβRII. Granulocytes comprised around 1% of the cell mass in KAT-4 carcinomas and their number was not changed after inhibition of TGF-β1 and -β3 (data not shown).

Inhibition of TGF-β1 and -β3 Modifies Vascular Morphology

The effects of Fc:TβRII on IFP in KAT-4 carcinomas may be due to changes in vascular function. This is based on the finding that inhibitors of the VEGF system lower tumor IFP and 'normalize' vascular function in carcinoma.[14,26] We therefore investigated potential effects of vessel maturation after treatment of KAT-4 carcinoma with Fc:TβRII. Expression of NG2 protein was downregulated (Figure 2a), whereas αSMA expression was either unaffected or slightly upregulated (Figure 2a). The percentage of CD31-positive vessels that were also positive for αSMA was significantly increased in tumors treated with Fc:TβRII (Figure 2b, c). In addition, more αSMA-expressing extravascular cells were present in tumors treated with Fc:TβRII than with IgG_{2A} (arrows in Figure 2b). To investigate blood perfusion in KAT-4 carcinomas, tumor-bearing mice were injected with high molecular mass FITC-labeled dextran prior to killing. There was no significant difference between the number or distribution of perfused vessels (Figure 2f) in tumors treated with Fc:TβRII (65 ± 24 vessels per mm^2, $n=5$) and IgG_{2A} controls (65 ± 12 vessels per mm^2, $n=4$). Vessel integrity was investigated by semiquantitative analyses of the leakage of EBD.[27] In the circulation, EBD is irreversibly bound to albumin. EBD present in tissues, therefore, reflects albumin leakage from capillaries.[28] Treatment of mice bearing KAT-4 carcinomas with Fc:TβRII reduced EBD leakage in the carcinomas compared to IgG_{2A} treatment (Figure 2f). The significance of this difference was assessed by a grading procedure (Figure 2d) or by densitometric analysis (Figure 2e).

Together these data suggest that Fc:TβRII normalized blood vessels with regard to pericyte activation, α-SMA coverage and extravasation of albumin.

Inhibition of IL-1 Reduces Tumor IFP

The gene expression data, as well as immunohistochemical analyses, suggested that interference with TGF-β1 and/or -β3 modulated macrophages in KAT-4 carcinomas. Since IL-1β was reduced after treatment with Fc:TβRII and since it is secreted by activated macrophages, its potential role in maintaining a high IFP in KAT-4 carcinoma was investigated. Treatment of mice carrying KAT-4 carcinomas with rh-IL-1 Ra ($n=9$) significantly reduced IFP to a similar degree as treatment with Fc:TβRII ($n=15$; $P<0.05$) (Figure 3 and data from Lammerts *et al*[19]). Combined treatment of animals with Fc:TβRII and rh-IL-1 Ra ($n=7$) had no additive effect on IFP compared to any of the inhibitors alone (Figure 3).

The number of infiltrating macrophages was reduced by 43% to 453 ± 54 cells per mm^2 (9.5 ± 1.3% of total cellular density) after treatment with rh-IL-1 Ra ($n=4$) (cf Figure 1b). Furthermore, the fraction of MHC class II antigens expressing F4/80-positive macrophages was reduced by 28% in rh-IL-1 Ra-treated carcinomas compared to controls.

Inhibition of IL-1 had No Effect on Vascular Morphology

Whereas expression of NG2 protein was downregulated in KAT-4 carcinomas treated with Fc:TβRII, treatment with rh-IL-1 Ra did not decrease this expression (data not shown). Qualitative immunofluorescence analyses revealed no significant change in perivascular αSMA-expressing cells in

KAT-4 carcinomas treated with rh-IL-1 Ra compared to controls (data not shown). Furthermore, no significant change in the percentage of CD31 positive vessels that were also positive for αSMA was observed after treatment with rh-IL-1 Ra (Figure 4a). However, there was a trend for a decreased extravasation of albumin after treatment with rh-IL-1 Ra although this effect did not reach significance (Figures 4b and c).

Inhibition of TGF-β1 and -β3 or IL-1 did not Influence Angiogenesis

The microarray analyses of KAT-4 tumors showed no changes in expression of genes associated with vascular function. Furthermore, expressions of several mouse mRNAs encoding various markers of angiogenesis were similar in KAT-4 carcinomas from animals treated either with IgG_{2A}, Fc:TβRII or rh-IL-1 Ra (Figure 5a). Notably, the expression of human VEGF mRNA was similar in the different groups of carcinomas (Figure 5b). Production of VEGF by cultured KAT-4 cells was ~0.2 ng/h/10^6 cells and this production was not affected by the addition of Fc:TβRII or rh-IL-1 Ra to the culture media (data not shown). Furthermore, levels of VEGF relative to total protein in extracts from KAT-4 carcinomas treated with Fc:TβRII or rh-IL-1 Ra were not different from the respective controls (data not shown).

Microvessel density and distribution within the viable zone was similar in carcinomas treated with Fc:TβRII ($n=4$), rh-IL-1 Ra ($n=6$) or IgG_{2A} ($n=4$) when assessed by morphometry of CD31 positive structures (Figure 5c). Similar results were obtained when vessels were visualized by staining for the 'panendothelial cell antigen' (data not shown). Laminin was expressed in vascular basement membranes and this expression was not qualitatively affected by either of the two inhibitors (data not shown). Expression of VEGFR-3 and lymphatic vessel endothelial HA-receptor-1 were not detectable in the viable zone of tumors treated with Fc:TβRII, rh-IL-1 Ra or IgG_{2A} (data not shown).

Inhibition of TGF-β1 and -β3 Augments Efficacy of Doxorubicin

The potential of treatment with Fc:TβRII to augment chemotherapy was investigated. Animals with KAT-4 carcinomas were pretreated with 1 mg/kg of Fc:TβRII ($n=4$), or IgG_{2A} ($n=4$). Starting 10 days after the administration of Fc:TβRII animals were treated for 2 weeks with doxorubicin in a dose

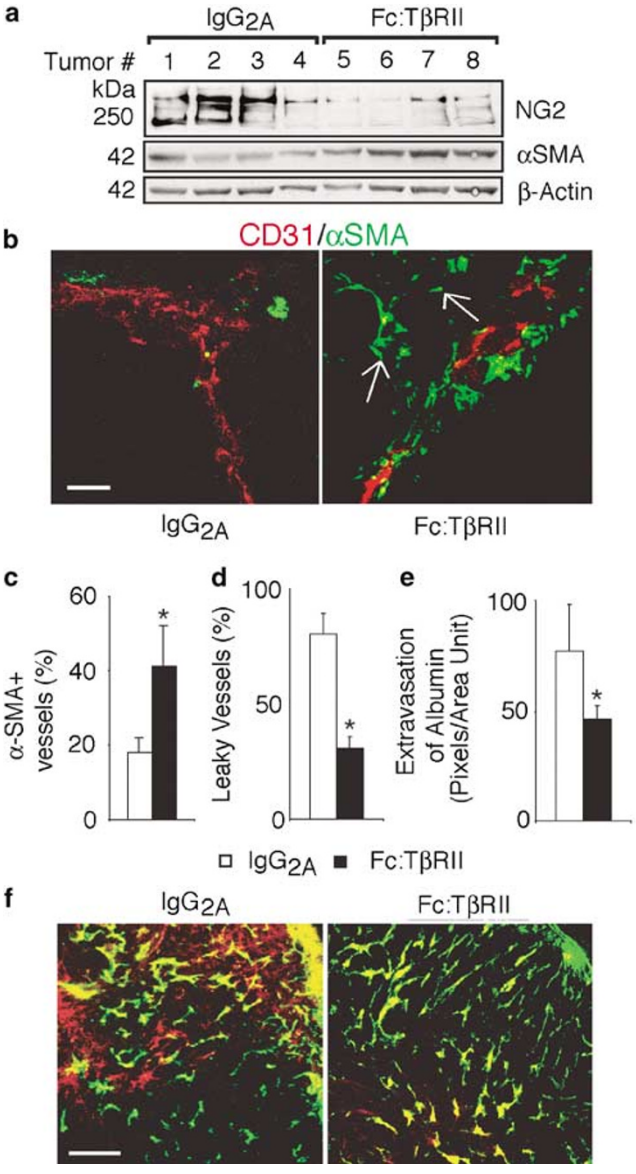

Figure 2 Fc:TβRII matured blood vessels and reduced albumin extravasation in KAT-4 carcinomas. (**a**) Immunoblot analysis of KAT-4 carcinoma tissue for mural cell markers expression. Tumor tissue samples were obtained from mice that had received a single injection of Fc:TβRII (10 mg/kg) ($n=4$) or IgG_{2A} ($n=4$) 10 days prior to harvest of carcinoma. β-Actin was used as a control for loading. Double immunofluorescence and confocal microscopy were used (**b**) to evaluate αSMA expression (green) in cells associated with CD31-positive tumor vessels (red). White arrows indicate on αSMA-expressing cells localized in tumor interstitium. Bar, 20 μm. (**c**) Quantification of vessels containing αSMA-positive cells in KAT-4 carcinoma treated with Fc:TβRII. Tumor sections were stained by double immunofluorescence for CD31 and αSMA. The percentage of vessels covered by αSMA positive cells out of total vascular density was quantified in low power fields (tumors from three animals per group, investigated area per tumor 3–6 mm^2). Densitometric and semiquantitative analysis of EBD vascular leakage (**d,e**) in KAT-4 carcinomas treated with Fc:TβRII ($n=5$) and IgG_{2A} ($n=5$). Leakage of tumor vessels for albumin was assessed using an EBD permeability assay. Perfused vessels were visualized by FITC-Dextran (2000 kDa). Tumor tissue samples were analyzed by microscopy as described in Materials and methods. One area unit corresponds to 69 μm^2. In (**d**) data are presented as percentage of vessels with high leakage for EBD. In (**f**) leakage of tumor vessels for EBD is shown in red. Perfused area of tumor tissue was assessed by analyses of FITC-Dextran distribution (green). Bar, 200 μm. * indicates $P<0.05$ from IgG_{2A} control.

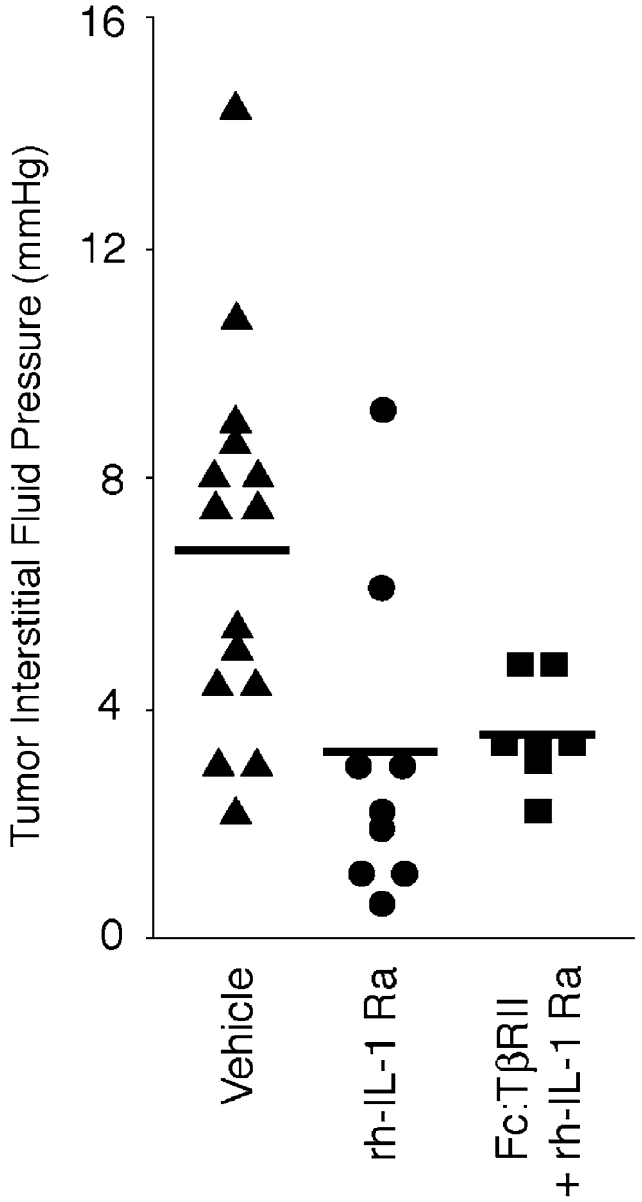

Figure 3 Inhibition of IL-1 lowered tumor IFP in KAT-4 carcinomas. Administration of rh-IL-1 Ra twice daily for 10 days with 7.5 mg/injection to KAT-4 carcinoma-bearing mice lowered tumor IFP by around 50%, that is, to the similar degree as Fc:TβRII alone.[19] There was no additive effect on tumor IFP observed after combined treatment with Fc:TβRII (a single injection at a dose of 10 mg/kg) and rh-IL-1 Ra.

pretitrated to have minimal effects on tumor growth. Control animals received a single injection of Fc:TβRII alone at a dose of 1 mg/kg ($n=4$). The dose of 1 mg/kg of Fc:TβRII was chosen since it was the lowest dose of Fc:TβRII which reduced IFP in KAT-4 carcinoma.[19]

The antitumor effect of doxorubicin was significantly greater after pretreatment with Fc:TβRII compared to IgG_{2A} (Figure 6a). In contrast, the growth inhibitory effect of doxorubicin on cultured KAT-4 cells was not influenced by the presence of either TGF-β1 or Fc:TβRII (Figure 6b).

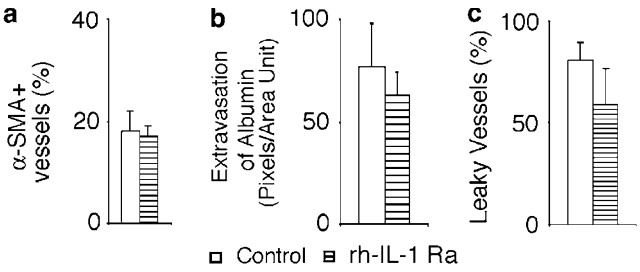

Figure 4 Effects of rh-IL-1-Ra on blood vessel maturation and albumin extravasation. In (**a**) quantification of vessels containing αSMA-positive cells in KAT-4 carcinoma treated with rh-IL-1 Ra twice daily with 7.5 mg/injection for 10 days ($n=4$). Tumor sections were stained by double immunofluorescence for CD31 and αSMA. Leakage of tumor vessels for albumin was assessed using an EBD permeability assay. In (**b**) and (**c**) densitometric and semiquantitative analysis of EBD vascular leakage in KAT-4 carcinomas treated with rh-IL-1 Ra ($n=4$) and IgG_{2A} ($n=5$). Perfused vessels were visualized by FITC-Dextran (2000 kDa). Tumor tissue samples were analyzed by microscopy as described in Materials and methods. One area unit corresponds to 69 μm^2. In (**c**) data are presented as percentage of vessels with high leakage for EBD.

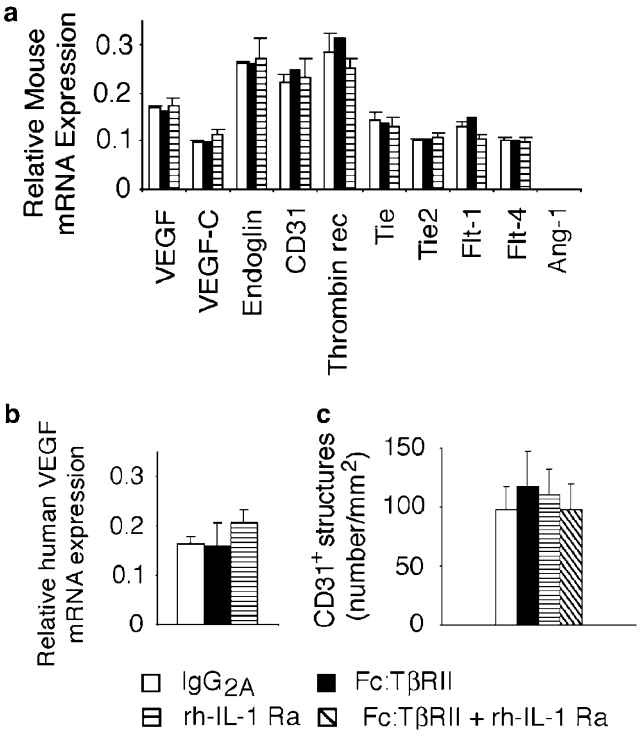

Figure 5 Fc:TβRII and rh-IL-1 Ra had no effects on angiogenesis. (**a**) Expression of a set of mouse genes involved in angiogenesis was investigated in KAT-4 carcinomas treated with Fc:TβRII ($n=2$), IgG_{2A} ($n=3$) or rh-IL-1 Ra ($n=3$) (**b**) Carcinoma RNA was extracted and subjected to RPA 10 days after a single injection of Fc:TβRII (10 mg/kg) or IgG_{2A} (10 mg/kg) or after treatment with rh-IL-1 Ra for 10 days (7.5 mg/injection, twice daily). RPA analyses of levels of human VEGF (KAT-4 cells) mRNA. (**c**) Microvessels were identified by immunohistochemistry with anti-CD31/PECAM-1 Mab in KAT-4 carcinomas treated with Fc:TβRII ($n=4$), rh-IL-1 Ra ($n=6$), Fc:TβRII combined with rh-IL-1 Ra ($n=4$) or IgG_{2A} ($n=4$). The density of CD31-positive structures was counted and expressed as number per mm^2 of tumor viable zone (5–22 vision fields, $\times 200$).

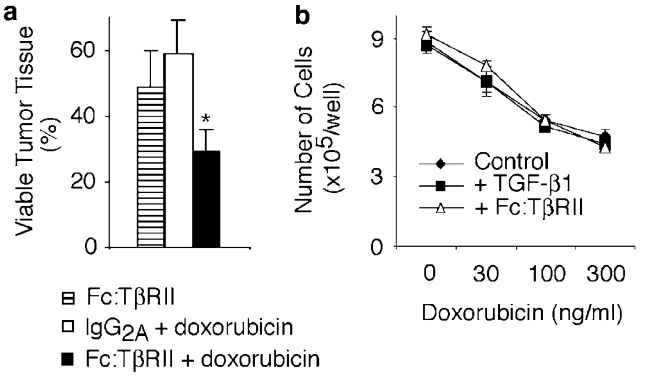

Figure 6 Pretreatment with Fc:TβRII increased efficacy of doxorubicin in KAT-4 carcinomas *in vivo*. In (**a**) KAT-4 tumor-bearing mice were pretreated with a single injection of Fc:TβRII (1 mg/kg) or IgG$_{2A}$. After 10 days, animals received doxorubicin at a dose of 3 mg/kg every second day during a two week period. Control animals received a single injection of Fc:TβRII at a dose of 1 mg/kg. Pretreatment with Fc:TβRII increased treatment efficacy of doxorubicin as evident by a reduction of KAT-4 viable tumor tissue. In (**b**) influence of addition of Fc:TβRII (100 nM) or TGF-β1 (10 ng/ml) to cultured KAT-4 cell on the growth inhibitory effects of doxorubicin. * indicates $P<0.05$ from IgG$_{2A}$ controls.

Discussion

The present data suggest that carcinoma-associated macrophages are involved in the regulation of IFP in experimental carcinoma. First, analyses of global gene expression patterns in KAT-4 carcinoma revealed that genes expressed by macrophages constituted a major group of genes that were downregulated after interference with TGF-β1 and -β3. Genes encoding MHC class II antigens, mannose receptors, IL-1β, S100 calcium-binding protein A9 (MRP-14) and the chemokine MCP-2 were downregulated. Since MHC class II antigens expression could only be positively identified in F4/80-positive macrophages, the downregulation of MHC class II antigens strongly suggests that macrophages are targeted by Fc:TβRII. Second, the number of intratumoral macrophages decreased after administration of Fc:TβRII, an effect coinciding with the lowering of tumor IFP. The reduction in macrophage numbers after treatment with the TGF-β inhibitor is in line with the well-established function of TGF-β1 as a chemoattractant for monocytes.[29,30] Third, the specific IL-1 inhibitor, rh-IL-1 Ra reduced IFP in KAT-4 carcinoma. Macrophages are major producers of secreted IL-1β in reactive tissues[31] and cultured KAT-4 cells secreted neither IL-1α nor -1β (data not shown). The expression of mouse IL-1α mRNA was low in KAT-4 carcinomas, suggesting that the effects of rh-IL-1 Ra on tumor IFP were due to inhibition of IL-1β. TGF-β induces IL-1β mRNA expression by cultured human monocytes,[29] a finding in line with the present result that inhibition of TGF-β1 and -β3 reduced IL-1β mRNA in KAT-4 carcinomas. In addition, treatment with the anti-inflammatory drug dexamethasone reduced macrophage density, expression of MHC class II antigens by macrophages and lowered IFP in KAT-4 carcinoma (data not shown). It is noteworthy that inhibitors of several growth factors or cytokines that are produced by activated macrophages, such as PDGF,[9] TGF-β1 and -β3,[19] IL-1 (present study) and VEGF[10] lower IFP in experimental carcinoma.

Expression of MHC class II antigens and mannose receptors by macrophages serve as markers of activation of these cells.[32] Fc:TβRII markedly downregulated class II expression by macrophages in KAT-4 carcinomas demonstrating that this inhibitor deactivated or, alternatively inhibited the activation of intratumoral macrophages. Both rh-IL-1 Ra and Fc:TβRII reduced the number of macrophages by $\sim$30–40% in KAT-4 carcinoma tissue, but no linear correlation between macrophage numbers and KAT-4 carcinoma IFP could be established (data not shown). Based on these notions, it therefore seems plausible that macrophage activation rather than number is important for their putative effects on tumor IFP.

Microvessel density in KAT-4 carcinomas was not affected by treatment with either Fc:TβRII or rh-IL-1 Ra. These findings show that the lowering of tumor IFP was not due to antiangiogenic effects of these inhibitors. However, treatment with Fc:TβRII significantly decreased extravasation of albumin in the carcinomas. A reduced protein leakage presumably reflects a normalization or maturation of the carcinoma vasculature. The decrease in NG2 expression, a marker of activated pericytes,[24,33,34] thus likely reflected a change in pericyte phenotype towards one more resembling that prevalent in normal and mature microvessels. The higher percentage of CD31 positive vessels containing αSMA-positive cells also favors the notion of a maturation of blood vessels in KAT-4 carcinomas from mice treated with Fc:TβRII. These findings speak in favor of a mechanism for IFP lowering by Fc:TβRII involving maturation of tumor blood vessels in KAT-4 carcinoma. Inhibition of IL-1 reduced IFP to a similar degree as Fc:TβRII but had less pronounced or no effects on the parameters for blood vessel maturation that were investigated. Furthermore, inhibition of IL-1 reduced albumin extravasation albeit this effect was not statistically significant. It is thus possible that Fc:TβRII and rh-IL-1 Ra lower tumor IFP by different mechanisms. Alternatively, the two inhibitors lowered IFP in KAT-4 carcinoma by a common mechanism involving subtle changes in blood vessel maturation. The finding that rh-IL-1 Ra reduced IFP in a nonadditive manner to Fc:TβRII is compatible with a common mechanism for lowering of carcinoma IFP by Fc:TβRII and rh-IL-1 Ra.

VEGF potently stimulates protein leakage from blood vessels[35] and activates nonendothelial vascular cells, for example, NG2 expression by pericytes in *in vivo* models of VEGF driven vasculogenesis.[36] The proangiogenic activity of IL-1α has been ascribed to a stimulation of VEGF production by

inflammatory cells.[37] Furthermore, treatment with inhibitors of the VEGF system reduces IFP, microvessel density and plasma protein leakage in experimental,[26] as well as human rectal carcinoma.[14] An attractive model is therefore that the effects of Fc:TβRII and rh-IL-1 Ra at least in part were due to a reduction of VEGF activity in KAT-4 carcinoma. The present findings do, however, not favor such a model. First and most importantly, neither Fc:TβRII nor rh-IL-1 Ra reduced microvessel density in KAT-4 carcinoma. This would be expected if inhibition of the VEGF system constituted a common mechanism for the IFP lowering by the two inhibitors. Second, levels of human and mouse VEGF mRNAs and protein were not changed in KAT-4 carcinomas treated with any of the two inhibitors. Third, VEGF production by cultured KAT-4 cells was not changed by the presence of Fc:TβRII or rh-IL-1 Ra (data not shown). Based on these findings it seems less likely that modulations of VEGF levels constituted a common mechanism for IFP lowering by Fc:TβRII or rh-IL-1 Ra.

Long-term presence of Fc:TβRII suppresses metastasis formation in experimental tumor models.[17,18] The present data showing that Fc:TβRII increases efficacy of chemotherapy should add to the clinical potential for adjuvant treatment of advanced malignancies using specific Fc:TβRII.

In conclusion, we present evidence suggesting that macrophages play a role in the generation of the pathologically elevated tumor IFP in a model for experimental carcinoma. Furthermore, our data propose that TGF-β1 and/or -β3 modulate macrophages in carcinoma.

Acknowledgements

This study was supported by grants from the Swedish Cancer Foundation, Gustaf V:s 80-årsfond (to KR) and Swedish Research Council (to NEH). Ms Ann-Marie Gustafson and Ms Annika Hermansson are gratefully acknowledged for technical assistance.

References

1 Tannock IF, Lee CM, Tunggal JK, *et al.* Limited penetration of anticancer drugs through tumor tissue: a potential cause of resistance of solid tumors to chemotherapy. Clin Cancer Res 2002;8:878–884.
2 Jain RK. Transport of molecules in the tumor interstitium: a review. Cancer Res 1987;47:3039–3051.
3 Jain RK. Physiological barriers to delivery of monoclonal antibodies and other macromolecules in tumors. Cancer Res 1990;50:814s–819s.
4 Wiig H, Tveit E, Hultborn R, *et al.* Interstitial fluid pressure in DMBA-induced rat mammary tumours. Scand J Clin Lab Invest 1982;42:159–164.
5 Rubin K, Sjöquist M, Gustafsson AM, *et al.* Lowering of tumoral interstitial fluid pressure by prostaglandin E_1 is paralleled by an increased uptake of ^{51}Cr-EDTA. Int J Cancer 2000;86:636–643.
6 Salnikov AV, Iversen VV, Koisti M, *et al.* Lowering of tumor interstitial fluid pressure specifically augments efficacy of chemotherapy. FASEB J 2003;17:1756–1758.
7 Emerich DF, Dean RL, Snodgrass P, *et al.* Bradykinin modulation of tumor vasculature: II. Activation of nitric oxide and phospholipase A2/prostaglandin signaling pathways synergistically modifies vascular physiology and morphology to enhance delivery of chemotherapeutic agents to tumors. J Pharmacol Exp Ther 2001;296:632–641.
8 Aukland K, Reed RK. Interstitial-lymphatic mechanisms in the control of extracellular fluid volume. Physiol Rev 1993;73:1–78.
9 Pietras K, Östman A, Sjöquist M, *et al.* Inhibition of platelet-derived growth factor receptors reduces interstitial hypertension and increases transcapillary transport in tumors. Cancer Res 2001;61:2929–2934.
10 Lee CG, Heijn M, di Tomaso E, *et al.* Anti-vascular endothelial growth factor treatment augments tumor radiation response under normoxic or hypoxic conditions. Cancer Res 2000;60:5565–5570.
11 Kristjansen PE, Boucher Y, Jain RK. Dexamethasone reduces the interstitial fluid pressure in a human colon adenocarcinoma xenograft. Cancer Res 1993;53:4764–4766.
12 Pietras K, Rubin K, Sjöblom T, *et al.* Inhibition of PDGF receptor signaling in tumor stroma enhances antitumor effect of chemotherapy. Cancer Res 2002;62:5476–5484.
13 Pietras K, Stumm M, Hubert M, *et al.* STI571 enhances the therapeutic index of epothilone B by a tumor-selective increase of drug uptake. Clin Cancer Res 2003;9:3779–3787.
14 Willett CG, Boucher Y, Di Tomaso E, *et al.* Direct evidence that the VEGF-specific antibody bevacizumab has antivascular effects in human rectal cancer. Nat Med 2004;10:145–147.
15 Heldin CH, Rubin K, Pietras K, *et al.* High interstitial fluid pressure—an obstacle in cancer therapy. Nat Rev Cancer 2004;4:806–813.
16 Roberts AB, Wakefield LM. The two faces of transforming growth factor β in carcinogenesis. Proc Natl Acad Sci USA 2003;100:8621–8623.
17 Muraoka RS, Dumont N, Ritter CA, *et al.* Blockade of TGF-β inhibits mammary tumor cell viability, migration, and metastases. J Clin Invest 2002;109:1551–1559.
18 Yang YA, Dukhanina O, Tang B, *et al.* Lifetime exposure to a soluble TGF-β antagonist protects mice against metastasis without adverse side effects. J Clin Invest 2002;109:1607–1615.
19 Lammerts E, Roswall P, Sundberg C, *et al.* Interference with TGF-β1 and -β3 in tumor stroma lowers tumor interstitial fluid pressure independently of growth in experimental carcinoma. Int J Cancer 2002;102:453–462.
20 Smith JD, Bryant SR, Couper LL, *et al.* Soluble transforming growth factor-β type II receptor inhibits negative remodeling, fibroblast transdifferentiation, and intimal lesion formation but not endothelial growth. Circ Res 1999;84:1212–1222.
21 Ain KB, Taylor KD. Somatostatin analogs affect proliferation of human thyroid carcinoma cell lines *in vitro*. J Clin Endocrinol Metab 1994;78:1097–1102.

22 Dahlman T, Lammerts E, Bergström D, *et al.* Collagen type I expression in experimental anaplastic thyroid carcinoma: regulation and relevance for tumorigenicity. Int J Cancer 2002;98:186–192.
23 Auffray C, Rougeon F. Purification of mouse immunoglobulin heavy-chain messenger RNAs from total myeloma tumor RNA. Eur J Biochem 1980;107: 303–314.
24 Sundberg C, Ljungström M, Lindmark G, *et al.* Microvascular pericytes express platelet-derived growth factor-β receptors in human healing wounds and colorectal adenocarcinoma. Am J Pathol 1993;143:1377–1388.
25 Reuterdahl C, Sundberg C, Rubin K, *et al.* Tissue localization of β receptors for platelet-derived growth factor and platelet-derived growth factor B chain during wound repair in humans. J Clin Invest 1993; 91:2065–2075.
26 Tong RT, Boucher Y, Kozin SV, *et al.* Vascular normalization by vascular endothelial growth factor receptor 2 blockade induces a pressure gradient across the vasculature and improves drug penetration in tumors. Cancer Res 2004;64:3731–3736.
27 Gratton JP, Lin MI, Yu J, *et al.* Selective inhibition of tumor microvascular permeability by cavtratin blocks tumor progression in mice. Cancer Cell 2003;4:31–39.
28 Wolman M, Klatzo I, Chui E, *et al.* Evaluation of the dye-protein tracers in pathophysiology of the blood-brain barrier. Acta Neuropathol (Berl) 1981;54:55–61.
29 Wahl SM, Hunt DA, Wakefield LM, *et al.* Transforming growth factor type β induces monocyte chemotaxis and growth factor production. Proc Natl Acad Sci USA 1987;84:5788–5792.
30 Derynck R, Akhurst RJ, Balmain A. TGF-β signaling in tumor suppression and cancer progression. Nat Genet 2001;29:117–129.
31 Dinarello CA. Biologic basis for interleukin-1 in disease. Blood 1996;87:2095–2147.
32 Gordon S. Alternative activation of macrophages. Nat Rev Immunol 2003;3:23–35.
33 Schlingemann RO, Rietveld FJ, de Waal RM, *et al.* Expression of the high molecular weight melanoma-associated antigen by pericytes during angiogenesis in tumors and in healing wounds. Am J Pathol 1990;136:1393–1405.
34 Stallcup WB. The NG2 proteoglycan: past insights and future prospects. J Neurocytol 2002;31:423–435.
35 Veikkola T, Karkkainen M, Claesson-Welsh L, *et al.* Regulation of angiogenesis via vascular endothelial growth factor receptors. Cancer Res 2000;60:203–212.
36 Witmer AN, van Blijswijk BC, van Noorden CJ, *et al. In vivo* angiogenic phenotype of endothelial cells and pericytes induced by vascular endothelial growth factor-A. J Histochem Cytochem 2004;52:39–52.
37 Salven P, Hattori K, Heissig B, *et al.* Interleukin-1α promotes angiogenesis *in vivo* via VEGFR-2 pathway by inducing inflammatory cell VEGF synthesis and secretion. FASEB J 2002;16:1471–1473.